Synthesis of copper-doped indium zinc sulfide nanosheets for high efficiency photocatalytic hydrogen production

Lei Chen[1], Zongwen Chen[2]
Luoyang Ship Material Research Institute, Luoyang, 471023, China
[1]Corresponding author
E-mail: [1]*chen9524006@163.com*, [2]*137106540@qq.com*

Received 13 March 2023; accepted 31 March 2023; published online 18 May 2023
DOI https://doi.org/10.21595/vp.2023.23272

63rd International Conference on Vibroengineering in Shanghai, China, May 18, 2023

Abstract. The excessive use of fossil energy has caused a series of environmental problems. Hydrogen is a green energy substitute for fossil energy, and photocatalytic hydrogen production is an effective means of hydrogen production. Indium zinc sulfide catalyst has great application prospect in the field of photocatalysis due to its advantages of high stability and visible light absorption. Based on this, Cu doped indium zinc sulfide nanosheets were prepared in this paper. Compared with pure indium zinc sulfide nanosheets, copper doped indium zinc sulfide nanosheets have better photocatalytic hydrogen production performance. The design and synthesis of photocatalytic hydrogen-producing catalyst has important guiding significance.

Keywords: Cu-doped, $ZnIn_2S_4$, nanosheets, photocatalytic, hydrogen production.

1. Introduction

In the process of industrial society, due to the excessive use of traditional energy, problems such as melting glaciers, environmental pollution and frequent natural disasters have become increasingly prominent [1-2]. Therefore, seeking energy saving and green alternative energy has become an urgent problem for people to solve. Hydrogen, as an ideal alternative energy source, can be produced by photocatalytic decomposition of water [3-5]. As we all know, the decomposition of water into hydrogen and oxygen is a non-spontaneous reaction process, the reaction equation is: $H_2O \rightarrow 1/2O_2+H_2$. In the standard state, it takes 237.2 kJ of energy to decompose 1 mol of water into hydrogen and oxygen. According to Nernst equation, the corresponding theoretical water decomposition voltage is 1.23 V. Therefore, the band gap energy of photocatalyst should be greater than 1.23 eV to achieve water decomposition. Due to the reduction potential and energy loss of reducing H^+ to H_2, the band gap of the semiconductor should preferably exceed 2 eV for photocatalytic hydrogen production [6-8]. $ZnIn_2S_4$ is suitable for photocatalytic hydrogen production due to its negative conduction ratio and band gap ranging from 2.06 eV to 2.85eV [9-11].

$ZnIn_2S_4$ has been widely concerned in the fields of photocatalytic hydrogen production, organic degradation, sterilization and so on, and has been extensively studied [10]. However, the low efficiency of photocarrier separation and the lack of active sites severely limit its photocatalytic performance. In order to overcome the inherent shortcomings of $ZnIn_2S_4$, great efforts have been made to further improve photocatalytic activity [12]. The structure design of photocatalyst is an effective way to improve the performance of photocatalyst. 2D $ZnIn_2S_4$ can selectively expose the (110) crystal surface, which is the most active crystal surface for photocatalytic water decomposition [13]. Moreover, ultra-thin nanoplates can produce longer-lived polishing carriers. Xie et al. synthesized $ZnIn_2S_4$ nanosheets with a thickness of about 6nm by hydrothermal method, and changed the electronic structure of the nanosheets through O doping to improve its photocatalytic reduction ability [14]. Element doping is to introduce impurity atoms into the lattice by chemical or physical methods to form defects or change the lattice type, thus

affecting the band structure and photocatalytic activity of the photocatalyst. Doping transition metal elements can change the optical properties of $ZnIn_2S_4$, such as Fe [15], Mo [16], etc. Gao et al. prepared iron-doped Zn composite material and investigated its photocatalytic degradation performance of 2, 4, 6-tribromophenol. The results show that the removal efficiency of Fe doped Zn for 2, 4, 6-tribromo-phenol is higher than that of pure $ZnIn_2S_4$. In the photocatalytic degradation reaction, the change of valence state of Fe ions effectively separated the photogenerated electrons and holes, and doping reduced the band gap of ZnIn2S4, thus expanding the range of light absorption [15].

Based on this, this paper prepared Cu-doped indium zinc sulfide nanosheets in order to improve the visible light catalytic hydrogen production performance of indium zinc sulfide. The results show that Cu-doped indium zinc sulfide nanosheets have been successfully synthesized, and compared with pure indium zinc sulfide nanosheets, cop-doped indium zinc sulfide nanosheets have better photocatalytic hydrogen production performance. This work expands the application of indium zinc sulfide catalyst in photocatalytic hydrogen production reaction.

2. Experiment

2.1. Synthesis of catalyst

2.1.1. Laboratory reagents

Zinc chloride (98 %), Indium chloride tetrahydrate (98 %), copper nitrate (98 %) and thioacetamide were purchased from Beijing Inokai Technology Co., LTD. All the ultrapure water used in the experiment was prepared by the ultrapure water machine Milli-Q Biocel.

2.1.2. Sample preparation

Pure indium zinc sulfide (ZIS) is first prepared. $ZnCl_2$ (0.2 mmol), $InCl_3 \cdot 4H_2O$ (0.4 mmol) and thioacetamide (1.8 mmol) were added to 30 m L deionized water. A uniform solution can be obtained by magnetic stirring for 30 min. Transfer the mixture to a 50 mL teflon-lined stainless steel hydrothermal reactor and react at 200 °C for 18 h. After the hydrothermal reactor cooled to room temperature, the products were centrifuged with distilled water and anhydrous ethanol in turn. Finally, the powder samples were dried in a vacuum drying oven at 60 °C for 12 h. The preparation process of Cu-doped indium zinc sulfide (Cu-ZIS) is as follows: $ZnCl_2$ (0.2 mmol), $Cu(NO_3)_2$ (0.04 mmol), $InCl_3 \cdot 4H_2O$ (0.4 mmol) and thioacetamide (1.8 mmol) were added to 30 m L deionized water. A uniform solution can be obtained by magnetic stirring for 30 min. Transfer the mixture to a 50 mL teflon-lined stainless steel hydrothermal reactor and react at 200 °C for 18 h. After the hydrothermal reactor cooled to room temperature, the products were centrifuged with distilled water and anhydrous ethanol in turn. Finally, the powder samples were dried in a vacuum drying oven at 60 °C for 12 h.

2.2. Performance and characterization of samples

X-ray powder diffraction is a characterization method to analyze the existence form and phase structure of each component in materials. In this paper, Cu-Kα ray is used under the condition of voltage 40 k V, in which the scanning range is 5-80°, scanning rate is 5°/min. All powder samples were detected by Lynx Eye array detector (one-dimensional detector). JEOL-2100F transmission microscope was used for Morphology and elemental analysis of the samples with an acceleration voltage of 200 kV. The method of characterization was to add the catalyst sample solution on the ultra-thin carbon film, then dried it fully and characterized it. X-ray photoelectron spectroscopy is used to study and analyze the elements on the surface of materials to determine the relative content, chemical valence state and existence form of each element. The vacuum degree of the analysis chamber is lower than 5.0×10^{-7} mBar, the excitation source is Mono Al Kα ray

($h\nu = 1486.6$e V), the working voltage is 12 k V, and the filament current is 6 mA. The binding energy of all elements was calibrated by C1s (284.8 eV). The atomic force microscope (AFM) studies the thickness of nanosheets by detecting very weak interatomic forces between the surface of the sample under test and a tiny force sensor.

In order to analyze the hydrogen production performance of the photocatalyst samples, the experimental steps were as follows: 50 mg composite photocatalyst was weighed into the reactor, and 100 m L of S2-/SO32- sacrificant solution was added (the composition was 0.25 mol/L Na_2S solution and 0.35mol/L Na_2SO_3 solution). The reaction solution was treated by ultrasonic for 10 min to ensure that the photocatalyst was evenly dispersed in the solution, and then the catalyst could receive light evenly. The Ar is continuously pumped in for 30 min to displace the air in the device. The simulated light source is a xenon lamp with a 300 W power and a filter ($\lambda \geq 420$ nm). The resulting gas is passed through a gas chromatograph equipped with a thermal conductivity detector (TCD, 13X column) to capture the amount of hydrogen produced. Samples were collected every 1 min in a cycle.

3. Results and discussion

3.1. Characterization and analysis of surface structure

High resolution transmission electron microscopy (HRTEM) were used to study the morphology of the prepared samples. Fig. 1 shows the morphologies of Cu-ZIS and ZIS. As shown in Fig. 1, both Cu-ZIS and ZIS exhibit smooth nanosheet morphology. The size of the nanosheets was irregularly distributed, which may be due to the fragmentation of the nanosheets caused by ultrasound during sample pretreatment. It is worth noting that the HRTEM images of Cu-Zis and ZIS are very similar, and no obvious CuS or Cu2S phases are observed, indicating that Cu is indeed doped in indium zinc sulfide to further investigate the thickness of the nanosheets, atomic force microscopy (AFM) was carried out. Isolated nanosheets of Cu-ZIS were selected for characterization. By AFM analysis, it is further determined to be a flat nanosheet structure with ultra-thin thickness, as shown in Fig. 2. From the corresponding height section view, it can be seen that the thickness of ultra-thin nanosheet is 6.312 nm, which is about 2.5 times of the thickness of $ZnIn_2S_4$ single crystal cell (2.47 nm) along [001] direction. It is further confirmed that the structure is two-dimensional ultra-thin nanosheet.

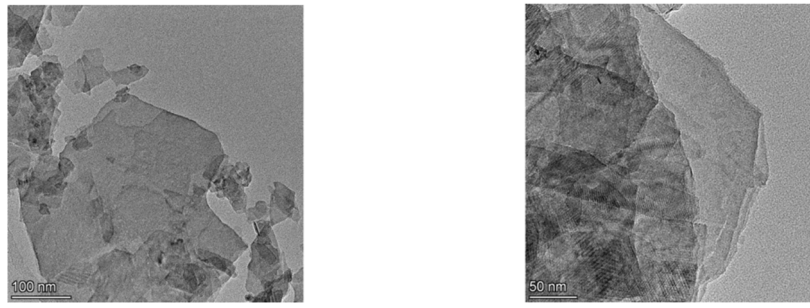

a) b)

Fig. 1. a) TEM image of Cu-ZIS, b) TEM image of ZIS

In order to understand the crystal structure of the catalyst, the samples were studied using X-ray diffractometer (XRD). XRD patterns of Cu-ZIS (black) and ZIS (red) are shown in Fig. 3. As shown in the Fig. 3, three strong characteristic diffraction peaks appear at 21.6°, 27.7° and 47.2°, corresponding to (006), (102) and (110) lattice planes of hexagonal phase $ZnIn_2S_4$ (JCPDS No. 72-0773). This shows that the catalyst synthesized is indeed indium zinc sulfide. In the XRD of Cu-ZIS, only the characteristic peaks of indium zinc sulfide are observed, and no CuS or Cu_2S

are observed, which further proves that Cu is doped in the lattice of indium zinc sulfide, rather than forming other substances. It is worth noting that the XRD peaks of Cu-ZIS and ZIS are almost the same, indicating that the introduction of Cu has no obvious effect on the lattice structure of indium zinc sulfide, which may be due to the fact that the atomic numbers of Cu and Zn are close and the atomic size difference is small. In Cu-doped indium zinc sulfide, Cu does not cause obvious lattice distortion at the position of replacing Zn.

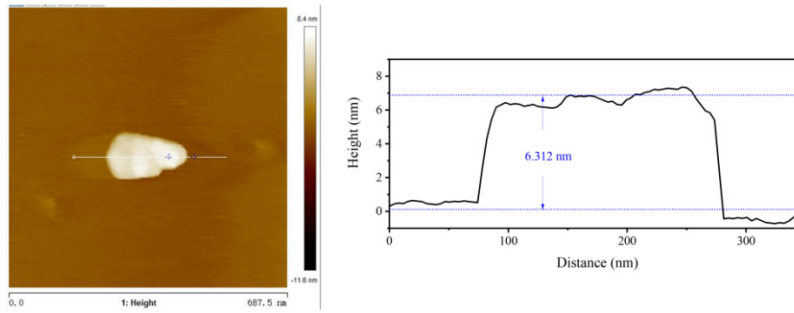

Fig. 2. AFM of Cu-ZIS

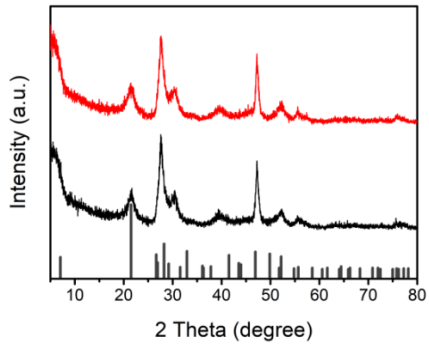

Fig. 3. XRD for Cu-ZIS (black) and ZIS (red)

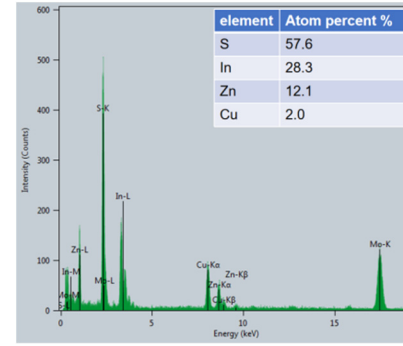

Fig. 4. EDS spectrum for Cu-ZIS

In the initial feed ratio, the ratio of Zn to Cu was 5:1, but under this reaction condition, Zn must react more easily than Cu to form indium zinc sulfide, meaning that the ratio of Cu to Zn in the final product Cu-ZIS should be less than 1:5. Energy dispersive spectroscopy (EDS) characterization was performed to investigate the specific incorporation amount of Cu in the reaction. As shown in the Fig. 4, it should be noted that the peak of Mo element appears in the figure, which is caused by the fact that the base used in the test contains Mo. Therefore, the element content obtained is the result of normalization after removing Mo element. The results show that the atomic ratio of Cu to Zn is about 1:6, and the atomic percentage of Cu is about 2 %, which is consistent with the expectation. In order to further investigate the bonding state of Cu, X-ray photoelectron spectroscopy of Cu-ZIS was performed. As shown in Fig. 5, the 2p orbital diagram of Cu shows an obvious characteristic peak of Cu^{+} or Cu^{0} (933 eV), rather than the characteristic peak of Cu^{2+} (934.5 eV), indicating that Cu exists in the form of Cu^{+} or Cu^{0} in Cu-ZIS. In view of the strong coordination effect of S on Cu, and the most stable state of Cu in $CuInS_2$ is Cu+, it is speculated that Cu exists in the form of Cu^{2+} initially, and in the hydrothermal process, Cu^{2+} is very likely to be reduced to the most stable form of Cu^{+}, rather than Cu^{0}.

Based on the above experimental data, we successfully synthesized Cu-doped indium zinc sulfide ultra-thin nanosheets. For comparison, ultra-thin indium zinc sulfide nanosheets have also been synthesized. In Cu-ZIS, the percentage of Cu atoms is about 2 %, which mainly exists in the form of Cu^{+}. Because Cu^{+} and Zn^{2+} have the same number of electrons and similar atomic size, the lattice structure of $ZnIn_2S_4$ does not change significantly after Cu replaces Zn, which indicates

that Cu+ can exist stably in $ZnIn_2S_4$ to some extent.

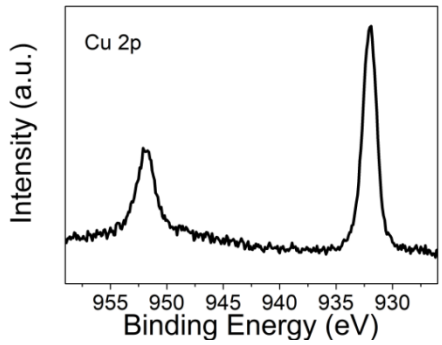

Fig. 5. XPS for Cu-ZIS

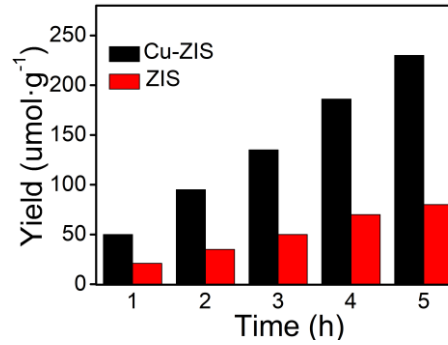

Fig. 6. The catalytic properties of hydrogen production

3.2. Characterization of catalytic properties of hydrogen production

Evaluation of surface catalytic reactions by photocatalytic hydrogen evolution. The results under visible light irradiation are shown in Fig. 6. In order to determine the performance of the photocatalyst accurately, the water decomposition experiment of Na_2S and Na_2SO_3 as sacrificial agent without chloroplatinic acid as cocatalyst was measured under visible light irradiation ($\lambda \geq 420$ nm). In Fig. 6, the hydrogen production rate of pure $ZnIn_2S_4$ is lower (23.5 $\mu mol \cdot h^{-1} \cdot g^{-1}$), which may be due to the rapid recombination of electrons and holes on the surface of $ZnIn_2S_4$. The hydrogen production rate of Cu-ZIS is 50.2 $\mu mol \cdot h^{-1} \cdot g^{-1}$, which is about twice that of ZIS. The above results indicate that the introduction of Cu heteroatoms can significantly improve the catalytic performance of indium zinc sulfide, which may be due to the fact that the introduction of Cu heteroatoms improves the hole separation efficiency of photogenerated electrons to a certain extent, thus improving the utilization efficiency of visible light, and electrons can effectively reduce H^+.

4. Conclusions

In this paper, Cu-doped $ZnIn_2S_4$ ultra-thin nano-sheets were prepared by hydrothermal synthesis. The microstructure and morphology of the catalyst were characterized by HRTEM, EDS, XRD and XPS. The results show that Cu-ZIS is an ultra-thin 6.3 nm nanosheet, which is about 2.5 times that of a single layer of indium zinc sulfide. Due to the strong binding ability of Zn and S under the reaction conditions, the atomic percentage of Cu in the catalyst is 2 %, which is significantly less than that in the original feed. Since Cu^+ and Zn^{2+} have the same number of electrons and similar atomic size, and exist stably in CuInS2, Cu exists in Cu-ZIS in the form of Cu^+. The presence of Cu heteroatoms significantly improves the photocatalytic hydrogen production performance of indium zinc sulfide, which may be due to the unbalanced distribution of electron clouds around Cu^+, which is favorable for photogenic electron hole separation.

Acknowledgements

The authors have not disclosed any funding.

Data availability

The datasets generated during and/or analyzed during the current study are available from the corresponding author on reasonable request.

Conflict of interest

The authors declare that they have no conflict of interest.

References

[1] J. Wang, S. Lin, N. Tian, T. Ma, Y. Zhang, and H. Huang, "Nanostructured metal sulfides: classification, modification strategy, and solar-driven CO_2 reduction application," *Advanced Functional Materials*, Vol. 31, No. 9, p. 2008008, Feb. 2021, https://doi.org/10.1002/adfm.202008008

[2] Z. Z. Feng, D. Mei, S. J. Zhu, and L. G. Wang, "Research progress of anode materials for primary magnesium-air batteries," *Development and Application of Materials*, Vol. 37, No. 6, pp. 12–21, 2022, https://doi.org/10.19515/j.cnki.1003-1545.2022.06.001

[3] M. G. Walter et al., "Solar water splitting cells," *Chemical Reviews*, Vol. 110, No. 11, pp. 6446–6473, Nov. 2010, https://doi.org/10.1021/cr1002326

[4] J. Corredor, M. J. Rivero, C. M. Rangel, F. Gloaguen, and I. Ortiz, "Comprehensive review and future perspectives on the photocatalytic hydrogen production," *Journal of Chemical Technology and Biotechnology*, Vol. 94, No. 10, pp. 3049–3063, Oct. 2019, https://doi.org/10.1002/jctb.6123

[5] A. Kubacka, M. Fernández-García, and G. Colón, "Advanced nanoarchitectures for solar photocatalytic applications," *Chemical Reviews*, Vol. 112, No. 3, pp. 1555–1614, Mar. 2012, https://doi.org/10.1021/cr100454n

[6] Q. Wang and K. Domen, "Particulate photocatalysts for light-driven water splitting: mechanisms, challenges, and design strategies," *Chemical Reviews*, Vol. 120, No. 2, pp. 919–985, Jan. 2020, https://doi.org/10.1021/acs.chemrev.9b00201

[7] B. Sun et al., "Synthesis of particulate hierarchical tandem heterojunctions toward optimized photocatalytic hydrogen production," Advanced Materials, Wiley, 2018.

[8] P. Ganguly et al., "2D nanomaterials for photocatalytic hydrogen production," *ACS Energy Letters*, Vol. 4, No. 7, pp. 1687–1709, Jul. 2019, https://doi.org/10.1021/acsenergylett.9b00940

[9] S. Shen, P. Guo, L. Zhao, Y. Du, and L. Guo, "Insights into photoluminescence property and photocatalytic activity of cubic and rhombohedral ZnIn2S4," *Journal of Solid State Chemistry*, Vol. 184, No. 8, pp. 2250–2256, Aug. 2011, https://doi.org/10.1016/j.jssc.2011.06.033

[10] W. Yang et al., "Layered crystalline ZnIn2S4 nanosheets: CVD synthesis and photo-electrochemical properties," Nanoscale, Royal Society of Chemistry (RSC), 2016.

[11] M. A. Sriram, P. H. Mcmichael, A. Waghray, P. N. Kumta, S. Misture, and M. A. Sriram, "Chemical synthesis of the high-pressure cubic-spinel phase of ZnIn2S4," *Journal of Materials Science*, Vol. 33, No. 17, pp. 4333–4339, Sep. 1998, https://doi.org/10.1023/a:1004424629498

[12] Y. Sun, S. Gao, F. Lei, and Y. Xie, "Atomically-thin two-dimensional sheets for understanding active sites in catalysis," *Chemical Society Reviews*, Vol. 44, No. 3, pp. 623–636, 2015, https://doi.org/10.1039/c4cs00236a

[13] X. Shi et al., "Ultrathin ZnIn2S4 nanosheets with active (110) facet exposure and efficient charge separation for cocatalyst free photocatalytic hydrogen evolution," *Applied Catalysis B: Environmental*, Vol. 265, p. 118616, May 2020, https://doi.org/10.1016/j.apcatb.2020.118616

[14] W. Yang et al., "Enhanced photoexcited carrier separation in oxygen-doped $ZnIn_2S_4$ nanosheets for hydrogen evolution," *Angewandte Chemie International Edition*, Vol. 55, No. 23, pp. 6716–6720, Jun. 2016, https://doi.org/10.1002/anie.201602543

[15] B. Gao, L. Liu, J. Liu, and F. Yang, "Photocatalytic degradation of 2,4,6-tribromophenol over Fe-doped ZnIn2S4: Stable activity and enhanced debromination," *Applied Catalysis B: Environmental*, Vol. 129, pp. 89–97, Jan. 2013, https://doi.org/10.1016/j.apcatb.2012.09.007

[16] F. Xing, Q. Liu, and C. Huang, "Mo-doped $ZnIn_2S_4$ flower-like hollow microspheres for improved visible light-driven hydrogen evolution," *Solar RRL*, Vol. 4, No. 3, p. 1900483, Mar. 2020, https://doi.org/10.1002/solr.201900483